Available online at www.sciencedirect.com
ScienceDirect
Tetrahedron
Tetrahedron 63 (2007) 9903–9914

Four classes of structurally unusual peptides from two marine-derived fungi: structures and bioactivities

Claudia M. Boot,[a,b] Taro Amagata,[a] Karen Tenney,[a] Jennifer E. Compton,[a] Halina Pietraszkiewicz,[c] Frederick A. Valeriote[c] and Phillip Crews[a,b,*]

[a]*Department of Chemistry and Biochemistry, University of California, Santa Cruz, CA 95064, USA*
[b]*Department of Ocean Sciences, University of California, Santa Cruz, CA 95064, USA*
[c]*Henry Ford Health System, Department of Internal Medicine, Division of Hematology and Oncology, Detroit, MI 48202, USA*

Received 7 May 2007; revised 1 June 2007; accepted 12 June 2007
Available online 16 June 2007

Abstract—The structures and biological properties of peptides produced by two genera of marine-derived fungi, an atypical *Acremonium* sp., and a *Metarrhizium* sp., were explored. The *Acremonium* strain was isolated from a marine sponge and has previously been shown by our group to produce peptides from the efrapeptin and RHM families. The isolation and structural elucidation of the new linear pentadecapeptides efrapeptins Eα (**1**) and H (**2**) and *N*-methylated octapeptides RHM3 (**3**) and RHM4 (**4**) were carried out through a combination of 1D and 2D NMR techniques and tandem MS. Additional known efrapeptins E, F, and G and the known syctalidamides A and B were also isolated. The absolute configurations of **1**–**4** are proposed to be the same as the original compound families. The marine sponge-derived *Metarrhizium* sp. was shown to produce destruxin cyclic depsipeptides including A, B, B2, desmethyl B, E chlorohydrin, and E2 chlorohydrin. Efrapeptins Eα (**1**), F, and G each displayed IC_{50}s of 1.3 nM against H125 cells, and destruxin E2 chlorohydrin displayed an IC_{50} of 160 nM against HCT-116 cells. An initial therapeutic assessment suggested a continuous (168 h) exposure of at least 2 ng/mL, or a daily (24 h) exposure of at least 300 ng/mL for H125 cells treated with efrapeptin G, and a continuous (168 h) exposure of at least 190 ng/mL for HCT-116 cells treated with destruxin E2 chlorohydrin, will cause 90% tumor cell death in vitro.

1. Introduction

Marine-derived fungi have proven to be both biologically diverse and wide ranging in their production of biosynthetic products. At the end of 2006 there were more than 500[1–3] unique molecular structures discovered from this source that are divisible into most of the major natural product biosynthetic classes, including peptides. This pattern is beginning to mirror the situation for cultured terrestrial-derived fungi, which historically have been a source of compounds containing unusual amino acid residues including cyclic peptides, cyclic depsipeptides, and linear peptides.[4] The mining of marine-derived fungi for additional members of these compound classes was considered to be promising and was the stimulus for this project.

One intent of this study was to further expand our library of marine-derived bioactive and/or unusual peptides. Success was realized as four classes of peptides were isolated from the parallel investigation of two different marine sponge-derived fungi. Our initial report[5] described two unique highly *N*-methylated peptides, RHM1 and RHM2, from the culture of an atypical marine sponge-derived *Acremonium* sp., and the potently cytotoxic known polypeptide efrapeptin G accompanied these compounds. Continuing scrutiny of this atypical *Acremonium* (strain number 021172c) has now yielded nine compounds. These consisted of the re-isolation of efrapeptin G,[6] accompanied by additional peptides including known efrapeptins E and F,[6] new efrapeptins Eα (**1**) and H (**2**), new linear *N*-methylated RHMs, 3 (**3**) and 4 (**4**), and known cyclic *N*-methylated syctalidamides A and B.[7] The NMR data on an extract of a *Metarrhizium* sp. (strain number 001103) indicated the presence of amide residues and further purification afforded six known *N*-methylated cyclic depsipeptides of the destruxin family. We now describe the physical and biological activity properties of these 15 peptides.

2. Results and discussion

The most complex peptides encountered in this study were pentadecapeptides belonging to the efrapeptin class. The five efrapeptins (C–G) described to date, shown in Figure 1, range in molecular weight from 1606 to 1648 Da and are usually produced by strains of *Tolypocladium* fungi. The

Keywords: Marine-derived fungi; Efrapeptin; Destruxin; RHM.
* Corresponding author. Tel.: +1 831 459 2603; fax: +1 831 459 2935; e-mail: phil@chemistry.ucsc.edu

0040–4020/$ - see front matter © 2007 Elsevier Ltd. All rights reserved.
doi:10.1016/j.tet.2007.06.034

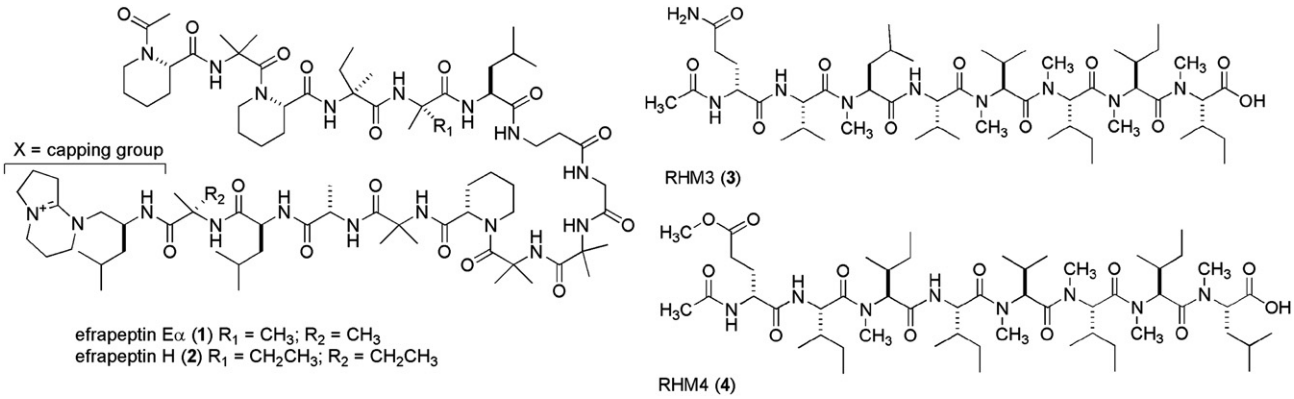

efrapeptin	*m/z* [M]$^+$, B_{10}, Y_5	amino acid number 1	2	3	4	5	6	7	8	9	10	11	12	13	14	15	cap
Eα (**1**)	1634.1, 945.6, 689.5	Ac-Pip	Aib	Pip	Iva	Aib	Leu	βAla	Gly	Aib	Aib	Pip	Aib	Ala	Leu	Aib	X
H (**2**)	1662.1, 959.6, 703.5	Ac-Pip	Aib	Pip	Iva	Iva	Leu	βAla	Gly	Aib	Aib	Pip	Aib	Ala	Leu	Iva	X
C[a]	1606.0, 931.6, 675.5	Ac-Pip	Aib	Pip	Aib	Aib	Leu	βAla	Gly	Aib	Aib	Pip	Aib	Gly	Leu	Aib	X
D[a]	1620.1, 931.6, 689.5	Ac-Pip	Aib	Pip	Aib	Aib	Leu	βAla	Gly	Aib	Aib	Pip	Aib	Gly	Leu	Iva	X
E	1634.1, 945.6, 689.5	Ac-Pip	Aib	Pip	Iva	Aib	Leu	βAla	Gly	Aib	Aib	Pip	Aib	Gly	Leu	Iva	X
F	1634.1, 951.6, 703.5	Ac-Pip	Aib	Pip	Aib	Aib	Leu	βAla	Gly	Aib	Aib	Pip	Aib	Ala	Leu	Iva	X
G	1648.1, 945.6, 703.5	Ac-Pip	Aib	Pip	Iva	Aib	Leu	βAla	Gly	Aib	Aib	Pip	Aib	Ala	Leu	Iva	X

[a] Calculated *m/z* values.

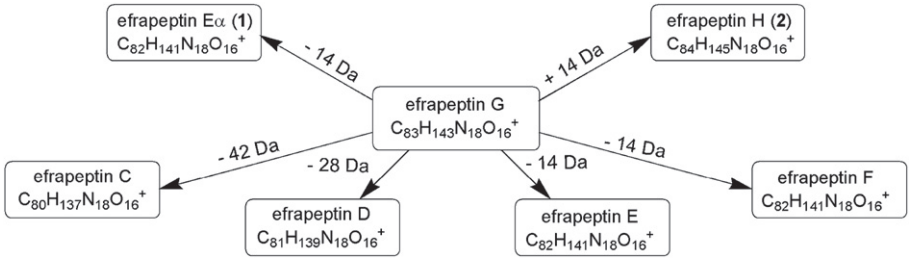

Figure 1. Amino acid composition and mass relationships of efrapeptins.

early literature associated with the efrapeptins can be tracked back to a 1978[8] report featuring an HPLC chromatogram with peaks for eight analogs labeled as efrapeptins A–H. At that point, no structures were proposed for the efrapeptins, and each compound was found to possess ATPase inhibitory activity. Three years later a partial structure for efrapeptin D appeared[9] and finally in 1991 the full structures of efrapeptins C—G were described.[6,10] However, complicating further analysis by others on this compound class was that the structural proofs employed an X-ray analysis on an efrapeptin D degradation product. Only partial NMR data were shown for efrapeptins C–G, while diagnostic FAB-MS *m/z* ion fragments were reported for efrapeptin F. Our recent report presented both comprehensive NMR and FAB-MS data sets for efrapeptin G providing benchmark data to facilitate characterizing an efrapeptin (including C–G).[5] The structures and physical properties for efrapeptins A and B have yet to be described, and only the molecular weight of efrapeptin H (1662 Da) has been published.[11,12]

Characterizing the full structure of an efrapeptin can be challenging. The first step in the process is to pinpoint the acylated pipecolic acid N-terminus and the charged $C_{13}H_{25}N_3$ bicyclic amine C-terminal capping group (capping group=X, see **1** and **2**). Also important is recognizing the patterns of additional structural variations known for this class relative to efrapeptin G. These relationships are summarized in Figure 1 and include: (a) switch of isovaline (Iva) with amino-isobutyric acid (Aib) at amino acid (AA) positions 4 and/or 15, and (b) exchange of alanine (Ala) with glycine (Gly) at AA-position 13.

The first goal of our additional investigation of the atypical *Acremonium* (strain number 021172c) was to re-supply efrapeptin G required for continuing the experimental therapeutic' evaluation. During the re-isolation of G, two new efrapeptins were encountered and recognized as being members of this class by observing, as noted above, the diagnostic NMR resonances of their terminal residues. One monumental challenge was that successive chromatographic steps were needed to complete the isolation work and they are outlined in Chart 1. At each step, progress was facilitated by obtaining disk diffusion bioassay data against human and murine tumor cell lines.[13] For example, pursuing the mycelial extract fraction (coded TFD) became a priority because the human lung non-small cell carcinoma (H125) cell lines displayed greater sensitivity versus that from the human lymphocytic leukemia (CEM) cell line. Eventually,

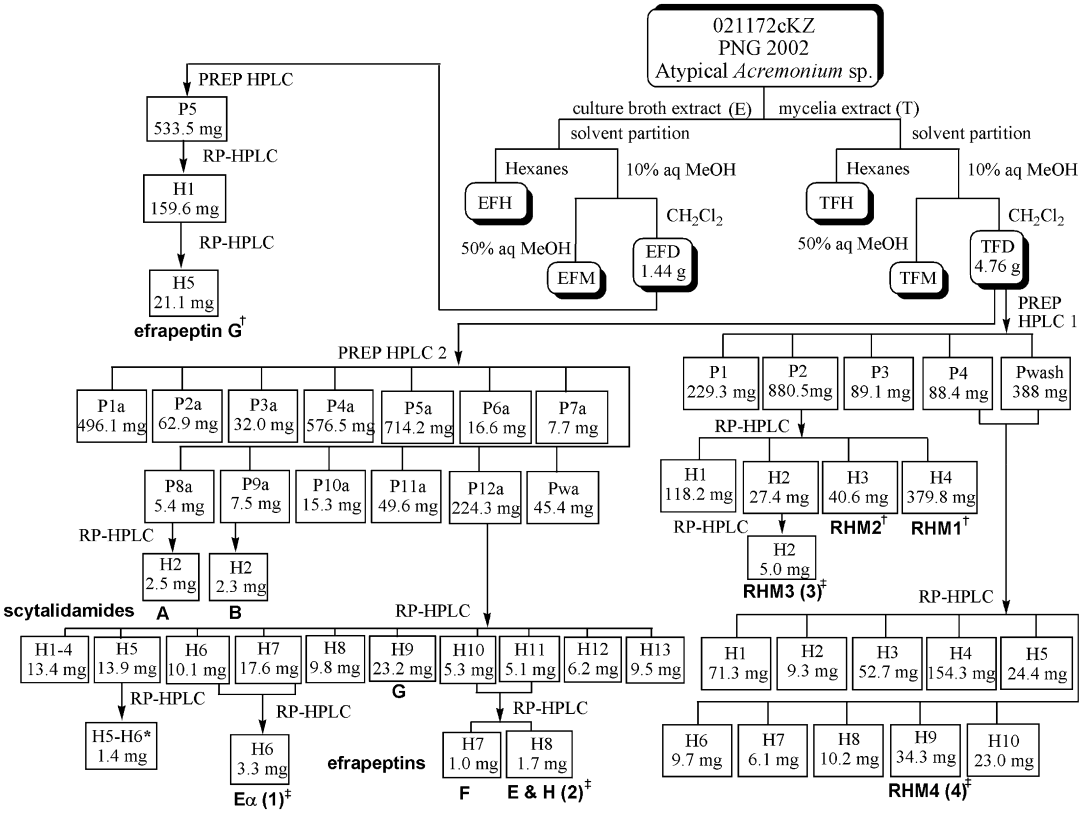

Chart 1. Isolation scheme affording efrapeptins, RHMs, and scytalidamides. †Compounds previously published from this extraction;[7] ‡new structures in this report. *Fraction was a mixture of three isomers with molecular weight (MW) 1606, and two isomers with MW 1620 (Fig. S5, Supplementary data).

an HPLC bioactive fraction (coded P12a) was concluded by LC–ESI-MS as having a mixture of new and known efrapeptins including E, Eα (**1**), F, G, and H (**2**). The main issue in characterizing the efrapeptins encountered was in fixing the location of side-chain amino acid methyl groups. As seen in Figure 1, relative to efrapeptin G the other four known analogs vary from it by a deficiency of 1–3 methyl groups. Further rounds of HPLC purification were carried out yielding pure efrapeptins Eα (**1**), F, and G. Though conditions could not be established to separate efrapeptins E and H (**2**), it was possible to analyze this pair using NMR and MS data.

The dereplication[14] of known efrapeptins, and the structural elucidation of new efrapeptins began by searching the ESI *m/z* data for the $[M]^+$ and ion fragments B_{10} and Y_5 summarized in Figure 1. The re-isolated sample of efrapeptin G displayed physical properties matching those we described previously. The structures of efrapeptin E (in a mixture with H (**2**), coded H8, Chart 1) and efrapeptin F (coded H7, Chart 1) were verified as being identical to those previously described after the extensive analysis of MS^n data sets (Fig. S6, Supplementary data). Masses equivalent to those of efrapeptins C and D were also observed in one HPLC fraction (coded H5–H6, Chart 1), however, multiple Y_5 fragments from MS^2 data demonstrated that this mixture was complex having at least three isomers from *m/z* 1606.0 (Y_5 *m/z*: 675.5, 689.5, 703.5) and two from *m/z* 1620.0 (Y_5 *m/z*: 689.5, 703.5) (Fig. S5, Supplementary data). Due to a limited amount of material (1.4 mg) efforts were not made to further purify this fraction.

The new compound named efrapeptin Eα (**1**) (HPLC peak purified by combining fractions coded H6 and H7) with *m/z* 1634.0756 supporting the MF $C_{82}H_{141}N_{18}O_{16}$ (Δ 1.1 mmu of calcd) was originally assigned as known efrapeptin E. This was based on the analysis of *m/z* ions for $[M]^+$, B_{10}, and Y_5. However, evidence that Eα (**1**) was distinct from efrapeptin E (present in the HPLC peak purified by combining fractions coded H10 and H11) first came from the ^1H NMR (Fig. 2) quartet at δ_H 4.04 (J=7.8 Hz). This was characteristic of an Ala α proton, not present in efrapeptin E but was observed in the ^1H NMR for efrapeptins F (AA-13) and G (AA-13).[5] The ion fragments observed by MS^n summarized in Figure 2 ultimately supported the AA constitution and sequence shown here for **1**, including the varying efrapeptin AA moieties (nos. 4, 5, 13 and 15). For example, MS^2 on the molecular ion (*m/z* 1634.1) of **1** resulted in fragment ions Y_{12} (*m/z* 1284.9) and Y_{11} (*m/z* 1185.8) confirming Iva as AA-4 and ion Y_{10} (*m/z* 1100.7) confirming Aib as AA-5. The identity of AA-13 was clarified via fragments from the MS^3 data: Y_3 (*m/z* 493.4) and MS^4: Y_2 (*m/z* 422.5) and AA-15 was assigned as Aib by the MS^4 data via fragment ions Y_1 (*m/z* 309.3) and Y_x (*m/z* 224.3, peptide capping group is X). The provisionally assigned ^1H NMR values are included herein (Table S1, Supplementary data) and agree with the structure established through MS. Most importantly, the ^1H NMR data set also rules out the possibility of replacing one of the leucines in **1** (at AA-6) with an Ile, as no doublet α-protons were observed. It is important to note that we assigned the standard peptide B and Y-type MS fragment ions in all spectra[15] along with ions from the loss of a peptide backbone oxygen.[16]

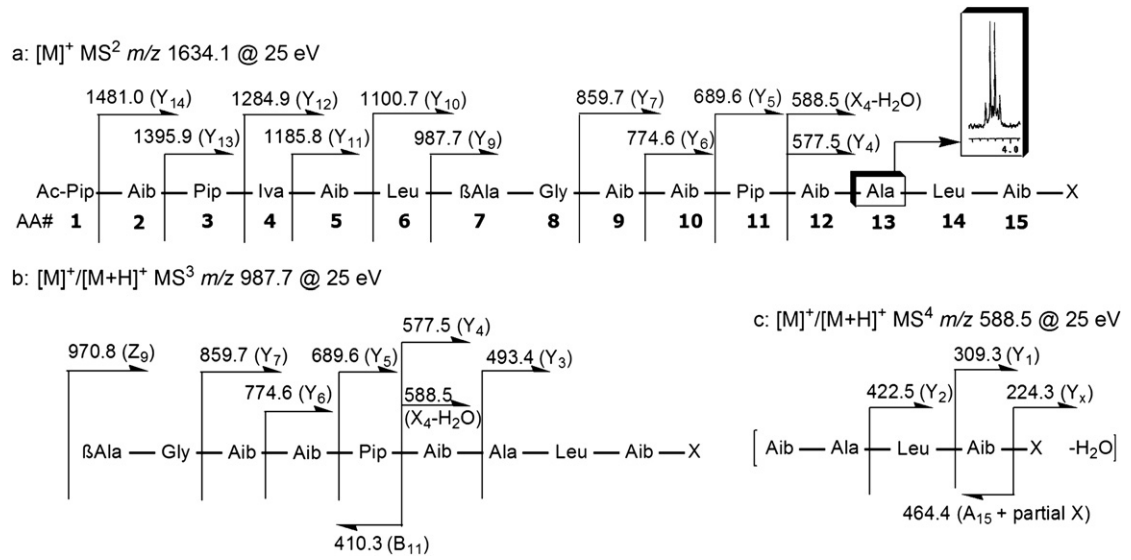

Figure 2. Observed MS^n *m/z* fragment ions (type) for efrapeptin Eα (**1**), $[M]^+$ 1634.1 with inset of ^1H NMR for Ala α proton and numbered amino acids.

Apparently, the charged C-terminus facilitates observing X–H_2O fragment ions rather than the normally observed B–H_2O ions that can occur via dehydration.

Similar to efrapeptin Eα (**1**), the structure of efrapeptin H (**2**) was also established through the use of extensive MS^n data. A confounding problem here was that **2** was present in small quantity and, as noted above, as a mixture with known efrapeptin E. The molecular formula of **2**, as $C_{84}H_{145}N_{18}O_{16}$, was established by the HR-ESI-MS *m/z* 1662.1078 $[M]^+$ (Δ 0.2 mmu of calcd), indicating the presence of one additional methyl group relative to efrapeptin G. The MS^n results were evaluated to probe for the differences at AA-4, -5, -13, and/or -15, and our first assumption was that the Aib at AA-5 of efrapeptin G was now an Iva. The MS^n experiments outlined in Figure 3 provided data to substantiate this postulate. The fragment ion at Y_{10} (*m/z* 1114.7) from MS^3 data (Fig. 3b) suggested that efrapeptins G and H (**2**) were identical from AA-6 through the X capping group. Alternatively, the +14 Da shift observed in the MS^3 data (Fig. 3c) at Z_{11} (*m/z* 1198.5) for **2** versus that expected for efrapeptin G provided the key to assign the Iva at AA-5. Additional MS data collected indicated that there were no multiple amino acid substitutions that would result in a structure for **2** with the same mass but different sequence of amino acids. These data included fragments Y_5 (*m/z* 703.5), Y_4 (*m/z* 592.4),

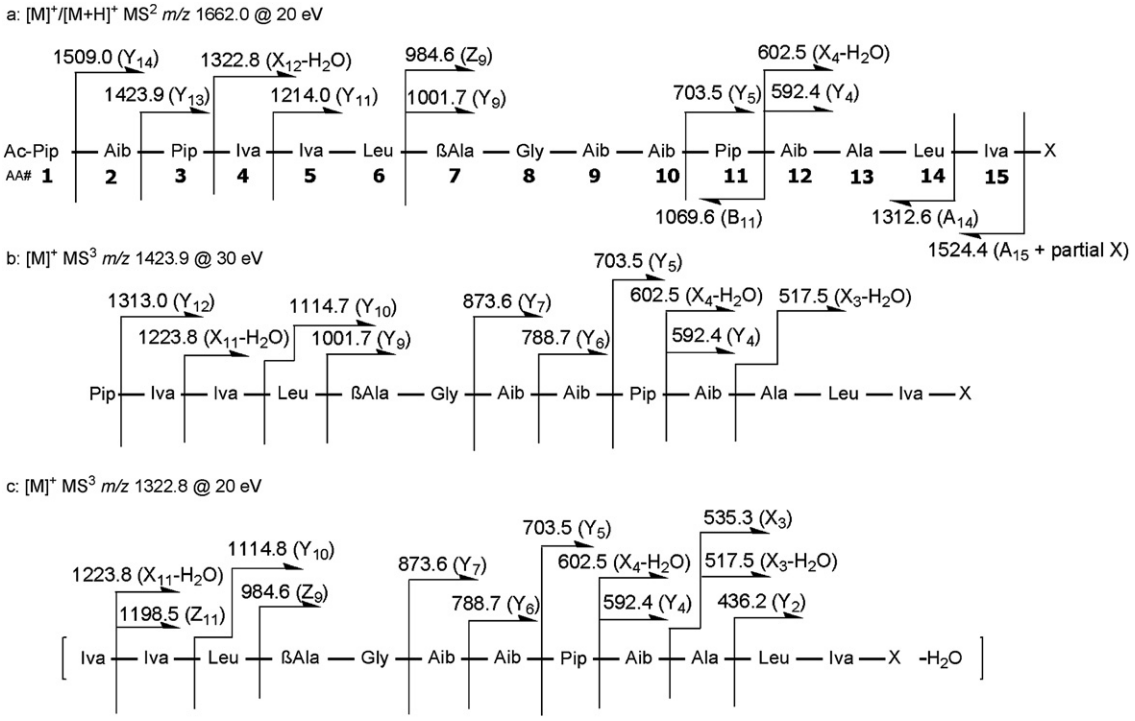

Figure 3. Observed MS^n fragment ions (type) for efrapeptin H (**2**), $[M]^+$ 1662.0.

X_3 (*m/z* 535.3), and Y_2 (*m/z* 436.2). Finally the *m/z* 1524.4 ($A_{15+partial\ X}$) fragment from the MS^2 experiment verified the C-terminal group.

Interestingly, the Y_8 fragment ion was not observed with ESI-MS for either **1** or **2**. Alternatively, fragmentation at the β-Ala–Gly junction was observed for the structurally similar neoefrapeptin A, but the peak was of very low intensity and this ion was not listed in the compound data.[17] The Y_8 ion was observed in the FAB-MS spectrum of our sample of efrapeptin G,[5] thus we are confident in the sequence of the new structures presented here.

The final step in the structural elucidation was to address the issue of absolute stereochemistry for the efrapeptins isolated here. All data in the literature indicate that each of the AAs in efrapeptin G possesses L stereochemistry[9,10] and the optical properties for our efrapeptin G ($[\alpha]_D^{28}$ −2.8 (*c* 0.07, $CHCl_3$)) match those of the literature.[6] Thus, we have provisionally assumed L stereochemistry for each of the AAs of **1** and **2** based on the parallel biosynthesis expected for these unique peptides versus that of efrapeptin G.

Our original report of metabolites from the 021172c *Acremonium* strain described the antibacterially active RHM1 and the inactive RHM2.[5] The RHMs are linear octapeptides containing five *N*–Me groups, having ~1000 Da molecular weight, and displaying four characteristic N-terminal acylium (B-type) fragments in ESI-MS. Two new compounds, RHM3 (**3**) and RHM4 (**4**), were purified during the bioassay-guided isolation of the H125 selective agents from the mycelial extract of the 20 L culture of strain 021172c. Shown in Figure 4 are the AA sequences and molecular mass relationship for all four peptides. The biggest hurdle in deciphering the NMR spectra of these linear peptides arose from the presence of multiple rotational isomers. The situation with RHM1 was ideal, as only one major form existed, while RHM2 had at least four rotational isomers. Discussed next are the parallelisms in the presence of rotamers for RHM3 (**3**) and RHM2 and the similarities observed for closely related RHM4 (**4**) and RHM1.

The structural elucidation of RHM3 (**3**), of formula $C_{51}H_{93}N_9O_{11}$ determined by HR-ESI-MS (*m/z* 1030.6878 $[M+Na]^+$, Δ 0.9 mmu of calcd), was greatly facilitated by a side-by-side comparison of its ^{13}C NMR data to that of RHM2. Akin to RHM2, it was possible to identify in **3**, 10 carbonyl carbons, 8 α carbons, 5 *N*-methyls, and 14 aliphatic methyls. The ^1H NMR data in Table 1 clearly showed one Gln, five *N*-methyl groups (δs 3.02, two at 3.07, and two at 2.93), three NHs (δs 8.28, 7.96, and 7.26), and eight α-protons (δs 5.17, 5.08, 4.77, 4.70, 4.52, 2 at 4.46, and 4.31). However, the presence of multiple rotamers prevented an accurate analysis of the multiplicities for these α-protons, which would have assisted in unraveling the amino acid similarities and differences between RHM2 and RHM3 (**3**). The ^{13}C NMR data of **3** versus RHM2 revealed Val (×2 or ×3), one Leu, and Ile (×3 or ×4). The count in favor of 3Val+3Ile+1Leu was derived by using MS and NMR data to probe the constitution of the aliphatic methyls. The gHMBC and gCOSY data shown in Figure 5 and Table 1 established the sequence homology between **3** and RHM2 at the first three AAs. The defining 2D NMR correlations were from H_3-1 to C-2, Ac–Gln_1 NH to C-2 and C-3, H-3 to C-4, Val_2 NH to C-4 and C-8, H-8 to C-9, and H_3-13 to C-9 and C-13. The three *N*–Me–Iles were assigned at AA-6–8 based on ESI-MS fragment ions B_5, B_6, and B_7 shown in Figure 5 and the additional data obtained were consistent with the placement shown for the remaining two isoleucines. The final issue of locating the unassigned *N*–Me at AA-5 rather than AA-4 was resolved by the MS^4 determination on *m/z* 662.4 providing ions at *m/z* 580.4 and 490.3 labeled in Figure 5 as fragments A_5 and A_4. Further affirming the final structure of **3** was the NMR assignment made for the side-chain Hs and Cs using TOCSY and COSY correlations along with comparisons to NMR data of RHM2 (Table 1).

The characterization of RHM4 (**4**) was confounded by overlapping ^1H NMR signals (Table 2) at 500 MHz, whereas an 800 MHz HMBC determination provided invaluable results. The molecular formula of **4**, $C_{54}H_{98}N_8O_{12}$ determined by HR-ESI-MS, *m/z* 1073.7254 $[M+Na]^+$ (Δ 5.7 mmu of calcd), differed from that of RHM1 by +COH and −N. The identification of AA-1 as Ac–Glu–*O*–Me in **4** versus the Ac–Glu present in RHM1 accounted for these differences and was substantiated by the gHMBC H_3-7 (δ 3.57, OCH_3) to C6 correlation shown in Table 2. Consistent with the parallel structures expected for this pair was that the ^1H NMR data of **4** included 3 *N*Hs (δ 8.30, 8.19 and 7.95), 5 *N*-methyls (δ 3.08, 3.02, 2 at 2.94, and 2.93), and 14 aliphatic methyls. The ^{13}C NMR resonances could be located for the remaining AAs as: AAs as: Ile X 5, Val X 1, and Leu X 1, and 2D NMR data shown in Figure 6 were used to establish the positions of each of the three *N*Hs and the five *N*-methyls. Similarly, gHMBC correlations (Fig. 6 and Table 2) were used to sequence the first five amino acids of **4**. The overlapping carbonyl signals of C-21 and C-40 complicated making an unequivocal connection

	mass	amino acid number 1	2	3	4	5	6	7	8
RHM3 (**3**)	1007.7	Ac-Gln	Val	*N*-Me-Leu	Val	*N*-Me-Val	*N*-Me-Ile	*N*-Me-Ile	*N*-Me-Ile-OH
RHM4 (**4**)	1050.7	Ac-Glu-*O*-Me	Ile	*N*-Me-Ile	Ile	*N*-Me-Val	*N*-Me-Ile	*N*-Me-Ile	*N*-Me-Leu-OH
RHM1	1035.7	Ac-Gln	Ile	*N*-Me-Leu	Ile	*N*-Me-Val	*N*-Me-Ile	*N*-Me-Ile	*N*-Me-Ile-OH
RHM2	1021.7	Ac-Gln	Val	*N*-Me-Leu	*N*-Me-Val	Ile	*N*-Me-Ile	*N*-Me-Ile	*N*-Me-Ile-OH

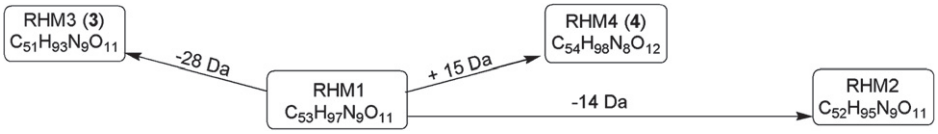

Figure 4. Amino acid composition and mass relationships of RHMs.

Table 1. ^{13}C (125 MHz), ^{1}H (500 MHz), and 2D NMR data for RHM3 (**3**) in DMSO-d_6

Amino acid	Position	^{13}C δ; type	^{1}H δ; mult. (J Hz)	gHMBC	gCOSY
Ac–Gln_1	1	22.4; CH_3	1.82; m	C2	
	2	169.0; C			
	NH[a]		7.96; d (8.5)	C2, C3	H3, H4,[k] H5[k]
	3	52.1; CH	4.31; ddd (5.5, 8.0, 13.5)	C7, C4, C5	Gln_1, NH, H4b
	4	28.5; CH_2	1.82; m, 1.66; m		H3
	5	31.6; CH_2	2.03; m		
	6	173.6; C			
	NH_2		7.26; m, 6.73; m	C6, C5	
	7	171.4; C			
Val_2	NH[a]		8.12; d (8.5)	C7	H8
	8[a]	52.5; CH	4.52; d (8.5)	C9, C12	Val_2NH, H9
	9	36.0; CH	1.82; m		H8
	10[b]	18.9; CH_3	0.77; m		
	11[b]	18.2; CH_3	0.77; m		
	12	172.1; C			
N–Me–Leu_3	13[c]	30.9; CH_3	3.02; s	C12	
	14	57.1; CH	5.08; dd (3.0, 10.5)	C19	H15a
	15	37.0; CH_2	2.20; m, 1.66; m		H14
	16	26.7; CH	1.82; m		
	17[d]	23.3; CH_3	0.77; m		
	18[d]	20.9; CH_3	0.77; m		
	19	170.1; C			
Val_4	NH[a]		8.28; d (8.0)		
	20[a,e]	53.9; CH	4.46; d (9.0)		H21
	21[f]	35.5; CH	1.82; m		H20
	22[b]	18.8; CH_3	0.77; m		
	23[b]	17.9; CH_3	0.77; m		
	24[g]	172.3; C			
N–Me–Val_5	25[c]	30.6; CH_3	3.07; s		
	26[a,e]	60.4; CH	4.70; d (11.0)		H27
	27[f]	35.5; CH	2.02; m		H26
	28[b]	18.6; CH_3	0.77; m		
	29[b]	17.5; CH_3	0.77; m		
	30[g]	171.9; C			
N–Me–Ile_6	31[c]	30.6; CH_3	3.07; s		
	32[a,e]	58.9; CH	4.77; d (11.0)		H33
	33[f]	32.6; CH	1.82; m		H32
	34[n]	24.0; CH_2	1.43; m, 1.20–1.04; m		
	35[i]	10.6; CH_3	0.77; m		
	36[j]	15.1; CH_3	0.77; m		
	37[g]	169.8; C			
N–Me–Ile_7	38[c]	29.9; CH_3	2.93; s		
	39[a,e]	55.3; CH	5.17; d (10.5)		H40
	40[f]	32.2; CH	2.04; m		H39
	41[n]	24.0; CH_2	1.43; m, 1.20–1.04; m		
	42[i]	10.5; CH_3	0.77; m		
	43[j]	14.9; CH_3	0.77; m		
	44[g]	169.7; C			
N–Me–Ile_8OH	45[c]	29.9; CH_3	2.93; s		
	46[a,e]	52.7; CH	4.46; d (9.0)		H47
	47[f]	30.1; CH	2.03; m		H46
	48[n]	23.5; CH_2	1.20–1.04; m		
	49[i]	10.2; CH_3	0.77; m		
	50[j]	14.5; CH_3	0.77; m		
	51[g]	169.8; C			
	OH		n.o.		

[a]Multiple signals appear due to rotation about amide bond. [b–j]Interchangeable signals. [k]Correlations from TOCSY spectra. n.o.: not observed.

between AA-3 and AA-4, so additional data used to resolve this point included the B_5 fragment ion at m/z 652.4, and the gHMBC correlation of the Ile NH to C-21/C-40. The B_5 ion dictated that AA-4 and AA-5 had a combined mass of 226.1 Da, which, along with the gHMBC correlation, required the sequence Ile–*N*–Me–Val. It was the 800 MHz NMR data (Table 2, Fig. S18, Supplementary data) and not the MS data that enabled the final sequencing amino acid residues 5–8. These gHMBC correlations were: (1) H-29 and H_3-34 to C-33 [connecting AA-5 to 6], (2) H-35 and H-42 to C-40 [affixing AA-6 to 7], and (3) from H_3-48 to C-49 [linking AA-7 to AA-8]. Although the signals of H_3-48 and H_3-41 overlapped (δ 2.94), 2D gHMBC correlations visible from H-42 and an *N*–Me (either H_3-41 or

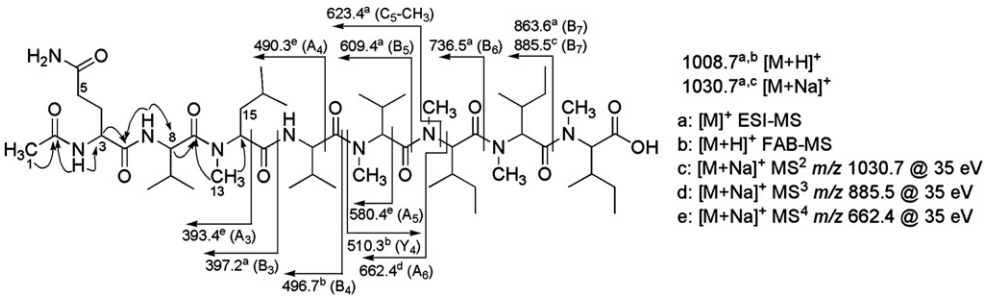

Figure 5. Key backbone gHMBC correlations and fragment ions from ESI-MS, FAB-MS, and MS^n experiments for RHM3 (**3**).

H_3-48) to C-47 showed that AA-7 cannot be at the C-terminus, so the *N*–Me–Leu must be AA-8. Given the close biosynthetic relationships among the RHMs the absolute stereochemistry shown here for **3** and **4** is based on an extension of that determined for RHM1.[5]

Two additional peptides were also isolated during our search for the mycelial extract fractions rich in efrapeptin G. These compounds were initially regarded as being potential unique efrapeptins as they eluted in fractions with enhanced polarity relative to all of the analogs discussed above. Eventually, through molecular formula-based dereplication, their identities were confirmed as known cyclic peptides, scytalidamide A[7] $[M+H]^+$ *m/z* 878.6, $C_{50}H_{67}N_7O_7$, and B, $[M+H]^+$ *m/z* 892.6, $C_{51}H_{69}N_7O_7$ (Chart 1, Scheme S1, Supplementary data), as their NMR properties (^1H and ^{13}C NMR data) exactly matched with those in the literature. It seemed unusual that our marine-derived *Acremonium* strain produced an identical set of metabolites found from a marine-derived *Scytalidium* strain. The Fenical laboratory generously provided their voucher material, which after re-culture in our laboratory was subsequently identified as an *Acremonium*.[18] Unanswered at this point is the extent to which this latter fungus is a source of efrapeptins and RHM type peptides. However, the scytalidamides share the unusual amino acid Aib with the efrapeptins and the *N*–Me groups in common with the RHMs.

Depsipeptides are another class of metabolites that were of interest in this project and fungal strains able to produce compounds of this class were obtained from our repository. A total of six cyclic depsipeptides of the destruxins class were re-isolated from a culture of the fungus *Metarrhizium* sp. (strain number 001103) obtained from a marine sponge. A large-scale (20 L) culture was investigated in order to pursue the bioactive metabolites (Fig. S1, Supplementary data). The components were isolated and included: destruxins A, B, B2, desmethyl B, E chlorohydrin, and E2 chlorohydrin (Scheme S1, Supplementary data), whose structures were confirmed by comparison of their ^1H and ^{13}C NMR data with that in the literature.[19,20]

The efrapeptins and destruxins share a common biological action against vacuolar-ATPase (vATPase).[21] In order to extend this comparison, efrapeptins Eα (**1**), F and G, and the six destruxin analogs were evaluated here for comparative bioactivities in a soft agar disk diffusion screen against human H125, HCT-116, CEM and murine C38, and CFU-GM cell lines.[13] Interestingly, efrapeptins Eα (**1**), F, and G each exhibited a similar IC_{50} value of 1.3 nM against H125 cells, indicating that the methyl group environment at Cα of AA-4, -13 or -15 has little impact on their cytotoxicity.

In addition to vATPase, efrapeptins are also known to inhibit mitochondrial F_1F_0-ATP synthase.[22] They were also recently shown to disrupt the interaction of ATP synthase and the heat shock protein 90 (Hsp90) complex.[23] The cellular function of the Hsp90 complex is to stabilize the newly produced or denatured proteins and the expression of Hsp90 is often upregulated in stressful environments, such as those found in tumor cells.[24] The H125 cell-based cytotoxicity observed for the efrapeptins may be due to the inactivation of Hsp90 through disruption of the Hsp90 complex–ATP synthase interaction. In support of this hypothesis, we found geldanamycin, a known Hsp90 inhibitor,[25] to have an IC_{50} against H125 cells of 4.5 nM, similar to that observed above for the three efrapeptins. Perhaps of relevance here was that the comparative responses of the efrapeptins and geldanamycin suggest the former may have further therapeutic potential. There are two geldanamycin analogs currently in clinical trials and show promise as multiple myeloma treatments.[26,27] While the enzymatic basis of the inhibition of ATP synthase by efrapeptins is well documented, the mechanism of cell-based bioactivity warrants further investigation. Interestingly, we observed resveratrol, another F_1F_0-ATP synthase inhibitor,[28] to have an H125 IC_{50} of 2200 nM, three orders of magnitude greater than that for the efrapeptins or geldanamycin. Although resveratrol has host of known biological activities,[29] its effect on the Hsp90-ATP synthase complex remains to be determined.

Additional comments need to be made about the SAR data for efrapeptins Eα (**1**), F, and G. In 1996, the crystal structure of the bovine F_1-ATPase was solved complexed with efrapeptin C. The crystal structural data indicated that the additional methyl groups of efrapeptins D–G could also be accommodated in the binding site,[22] thus differential bioactivity due to ATPase inhibition was unlikely. It should be noted that most of the efrapeptin-based biological studies are conducted with a varying mixture of efrapeptins due to the considerable difficulty involved in their purification.

Some of the destruxin analogs we tested showed an appealing bioactivity pattern in the disk diffusion assay. The data given in Figure 7 summarize the responses of two compounds, destruxins E and E2 chlorohydrin, which displayed selective cytotoxicity toward murine C38 cell line at the lowest concentration of 136 and 150 μM, respectively, while exhibiting no inhibition of CFU-GM cells. Against the human cell lines, destruxins A, B2, desmethyl B, and

Table 2. ^{13}C (125 MHz), ^{1}H (500 MHz), and 2D NMR data for RHM4 (**4**) in DMSO-d_6

Amino acid	Position	^{13}C δ; type	^{1}H δ; mult. (J Hz)	gHMBC	gCOSY	TOCSY
Ac–Glu–*O*–Me_1	1	22.4; CH_3	1.81; s	C2		
	2	169.0; C				
	NH		7.95; d (8.0)	C2, C3, C8	3	
	3	51.5; CH	4.36; dt (5.5, 8.0)	C4	NH, 4a	
	4	27.8; CH_2	1.73; m, 1.23; m		4a to 3	
	5	29.9; CH_2	2.27; m	C4, C6		
	6[a]	172.6; C				
	7	51.3; CH_3	3.57; s	C6		
	8	171.0; C				
Ile_2	NH		8.19; d (8.5)		9	15
	9	52.5; CH	4.51; t (9.0)	C10, C14	NH, 10	
	10	35.9; CH	1.81; m		9	
	11[b]	24.1; CH_2	1.44; m, 1.23; m			
	12[c]	10.5; CH_3	0.77; m			
	13[a]	14.9; CH_3	0.77; m			
	14	172.1; C				
N–Me–Ile_3	15	30.7; CH_3	3.08; s	C14, C16		Ile_2NH
	16	58.8; CH	4.78; d (11.0)	C14, C17	17	18a, 18b
	17	32.2; CH	1.81; m		16	
	18[b]	24.1; CH_2	1.73; m, 1.14; m 16			16
	19[c]	10.5; CH_3	0.77; m			
	20[a]	14.9; CH_3	0.77; m			
	21	169.8; C				
Ile_4	NH		8.30; d (8.0)	C21, C22	22	28
	22	52.7; CH	4.46; t (8.5)	C23, C27	NH, 23	24a, 24b
	23	35.5; CH	1.81; m		22	
	24[b]	24.0, CH_2	1.44, m; 1.07m			
	25[c]	10.4; CH_3	0.77; m			
	26[a]	14.7; CH_3	0.77; m			
	27	172.3; C				
N–Me–Val_5	28	29.9; CH_3	3.02; s	C27, C29		Ile_4NH
	29	57.2; CH	5.09; d (10.5)	C27, C30, C33[f]	30	
	30	26.7; CH	2.19; m		29	
	31	17.8; CH_3	0.77; m			
	32	18.7; CH_3	0.77, m			
	33	170.1; C				
N–Me–Ile_6	34[e]	31.1; CH_3	2.93; s	C33[f]		
	35	55.5; CH	5.16; d (11.5)	C40[f]	36	37a, 37b
	36	32.7; CH	2.01; m		35	
	37[b]	23.5; CH_2	1.14; m, 1.07; m			35
	38[c]	10.4; CH_3	0.77; m			
	39[a]	14.5; CH_3	0.77; m			
	40	169.8; C				
N–Me–Ile_7	41[e]	30.0; CH_3	2.94; s	C40[f]		
	42	55.2; CH	5.19; d (11.0)	C40,[f] C47[f]		
	43	32.7; CH	2.01; m			
	44[b]	23.4; CH_2	1.23; m, 1.14; m			
	45[c]	10.2; CH_3	0.77; m			
	46[a]	14.5; CH_3	0.77; m			
	47	170.2; C				
N–Me–Leu_8	48[e]	30.0; CH_3	2.94; s	C47[f]		
	49	53.8, CH	5.04; dd (12.5, 4.0)	C54[f]	50a	50a, 50b, 51
	50	36.4; CH_2	1.73; m		49	49
			1.56; ddd (4.0, 10.5, 14.5)			
	51	24.5; CH	1.23; m			49
	52	23.2; CH_3	0.77; m			
	53	20.8; CH_3	0.77; m			
	54[a]	172.7; C				
	OH		n.o.			

[a–e]Interchangeable carbon signals. [f]Correlations observed at 800 MHz. n.o.: not observed.

E chlorohydrin all demonstrated selective inhibition for the solid tumor cell lines, however, destruxin E chlorohydrin was the most potent inhibitor at 34 μM. The IC_{50} of the E chlorohydrin was subsequently measured and found to be 160 nM against HCT-116 cells.

The therapeutic assessment of efrapeptin G and destruxin E chlorohydrin continued with clonogenic evaluations designed to determine the exposure levels that would be required for positive in vivo cytotoxicity responses.[30] A therapeutic effect is defined by the amount of metabolite needed

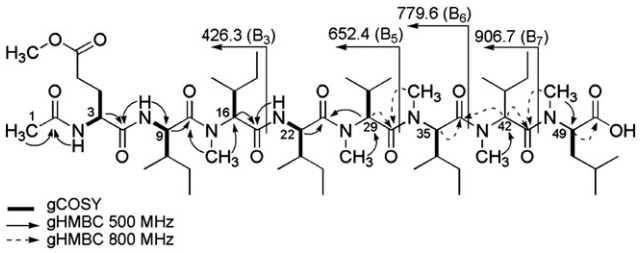

Figure 6. Key 2D NMR correlations and ESI-MS $[M]^+$ fragment ions (type) for RHM4 (**4**).

to kill 90% of the tumor cells (less than 0.1 in the surviving fraction, Fig. 8). Figure 8a highlights the results for efrapeptin G, indicating that a therapeutic effect against H125 cells would require a chronic exposure (168 h) at a concentration of 2.0 ng/mL or higher, or a bolus exposure (24 h) at a concentration of 300 ng/mL or higher. Presently, work is continuing to determine the maximum tolerated dose in mice (MTD), and to complete pharmacokinetic (PK) and in vivo studies. The results of the clonogenic study on destruxin E chlorohydrin shown in Figure 8b, indicated that only a chronic exposure (168 h) of 190 ng/mL or greater would yield the therapeutic effect against HCT-116 cells. The MTD for destruxin E chlorohydrin was established as 0.125 mg/mouse (6.25 mg/kg) and a PK study will be conducted at this dose.

3. Conclusions

The further therapeutic development of efrapeptin G, or any other efrapeptin studied here, as well as destruxin E chlorohydrin will require the re-supply of material. This could take place via two methods: (a) synthesis or (b) fermentation. Of the efrapeptins, only C has been the subject of total synthesis[31] and preparation of one unnatural analog has also been reported.[32] A similar set of circumstances exist for destruxin analogs such as A, B and desmethyl B, which have been prepared by chiral synthesis.[33] However, there have been no syntheses of the two destruxin chlorohydrins, E and E2, which were the most potently active of the destruxins isolated in this study (Fig. 7). Given this limited literature it will probably be more effective to isolate additional material through fermentation.

Four classes of peptides produced by marine-derived fungi were discussed here: linear *N*-methylated RHMs, α-alkylated efrapeptins, cyclic *N*-methylated scytalidamides, and

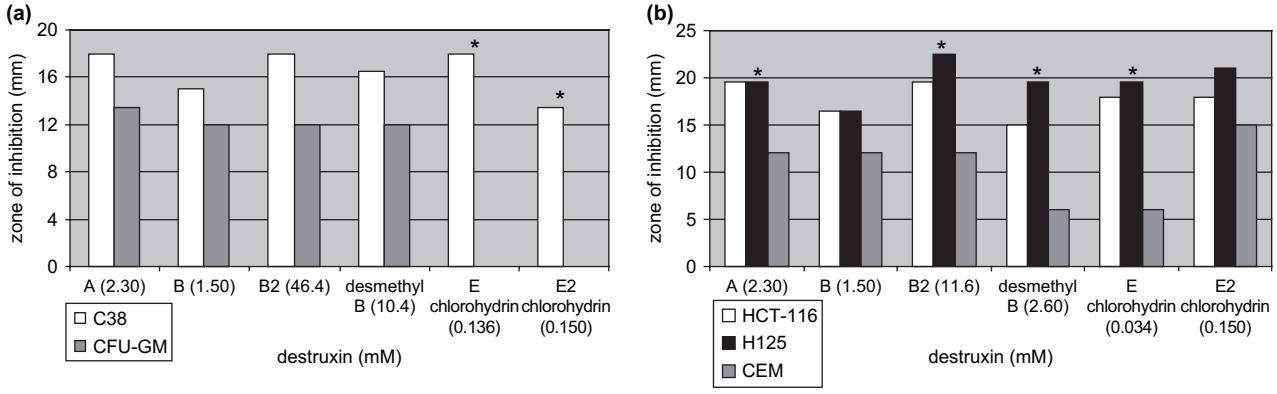

Figure 7. (a) Cytotoxicity of destruxins against murine cell lines. (b) Cytotoxicity of destruxins against human cell lines. *Selective cytotoxicity (>7.5 mm difference) for solid tumor cell lines. Murine cell lines: C38=colon adenocarcinoma, CFU-GM=bone marrow. Human cell lines: HCT-116=colorectal carcinoma, H125=lung non-small cell carcinoma, CEM=lymphocytic leukemia.

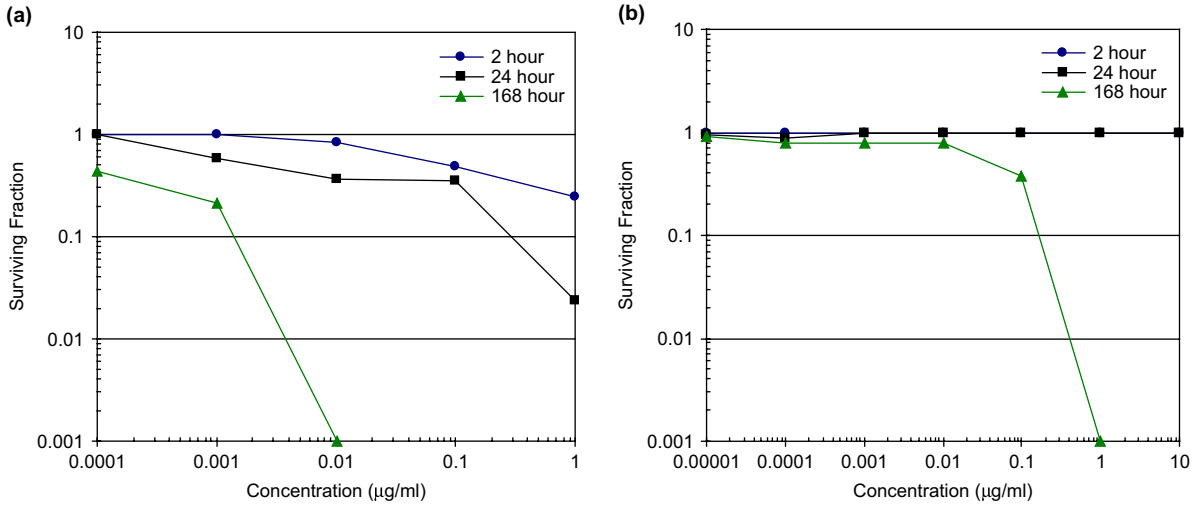

Figure 8. Concentration survival curve for clonogenic study of (a) efrapeptin G against H125 cells and (b) destruxin E chlorohydrin against HCT-116 cells.

the depsipeptide destruxins. Overall they exemplify the ideal structural properties of peptides with biological potential. The speed at which the structural elucidation of the RHMs could be completed varied according to the presence or absence of multiple rotamers. As noted above, two of these, RHM1 and RHM4 (**4**), adopt one major conformation whereas the other two, RHM2 and RHM3 (**3**), are observed to have a minimum of four conformations.[5] The presence of multiple amide bond rotamers is also observed for the aspergillamides,[34] linear *N*–Me tripeptides produced by a marine-derived *Aspergillus* sp.; and for the immunosuppressant cyclosporin A, an *N*–Me, 11 AA cyclic peptide, produced by species of *Trichoderma*.[35] The efrapeptins and destruxins show promise for further development of their cytotoxic properties. The RHMs, while not active in the assays examined here, may provide insights on the relevant question of how a mix of conformational isomers varies as a result of N-methylation.

4. Experimental section

4.1. General experimental procedures

The NMR spectra for **1**, **3**, and **4** were recorded at 500 or 600 MHz (^{1}H) and 125 MHz (^{13}C). High-resolution mass spectra were acquired with a bench top Mariner ESI-TOF and a Bruker ESI-microTOF-Q mass spectrometers, and MS^{n} experiments were conducted on a Thermo-Finnigin LTQ ESI-MS. Preparative RP-HPLC was performed using columns of 6 μm ODS; semi-preparative RP-HPLC was performed using columns of 5 μm ODS.

4.2. Biological materials

The basis for the classification of our 021172c strain of fungi has been previously described.[5] The strain provided by the Fenical laboratory (strain number CNC310) was taxonomically identified by molecular (ITS and D1/D2 regions of rDNA) and morphological methods by the University of Texas, Fungus Testing Laboratory. There was one mismatch in the molecular taxonomy sequence data of the two strains and the phenotypic examination showed that both were morphologically similar. The 001103 strain of fungi was separated from the sponge, *Pseudoceratina purpurea* (coll no 00103), collected in Fiji. It was taxonomically classified by morphological and molecular methods.[36] Each strain is maintained as cryopreserved glycerol stocks at UCSC.

4.3. Culture conditions

The large-scale (20 L) culture of strain 021172c was grown as previously reported,[5] in 3.5% Czapek-Dox media made with filtered Monterey Bay seawater-based media adjusted to pH 7.3 with shaking (150 rpm) for 21 days at room temperature (25 °C). The 20 L culture of strain 001103 was prepared in a medium containing 3.5% Czapek-Dox broth and 0.5% yeast extract in filtered Monterey Bay seawater (20 L) adjusted to pH 7.5 for 21 days at room temperature.

4.4. Biological assays

The disk diffusion assay has been formerly described.[5,13]

4.5. IC_{50} determinations

Determinations were carried out using our standard protocol as follows: either HCT-116 or H125 cells were plated at 5×10^{4} cells in T25 tissue culture flasks (Falcon Plastics, New Jersey) with 5 mL media RPMI 1640 (Cellgro, Virginia) supplemented with 15% BCS (Hyclone, Utah), 5% penicillin–streptomycin and 5% glutamine (Cellgro). Three days later (cells in logarithmic growth phase; 5×10^{5} cells/flask), test compound was added to the flasks to achieve concentrations ranging from 10 to 10^{-4} mg/mL. At day 3, the flasks were washed, trypsinized, centrifuged, and the cells counted for both viable and dead cells using 0.08% trypan blue (Gibco, Maryland). Viable cell number as a function of concentration was plotted and the IC_{50} values are determined by interpolation.

4.6. Efrapeptin G and destruxin E chlorohydrin clonogenic dose–response analysis

Clonogenic studies were carried out by our standard protocols using HCT-116 cells for destruxin E chlorohydrin and H125 cells for efrapeptin G. For these concentration- and time-survival studies, either HCT-116 or H125 cells were seeded at either 200 or 2000 cells in 60 mm culture dishes. Compound was added to the medium (RPMI+10% FBS) at concentrations of 1 mg/mL and 10-fold dilutions thereof. At either 2 or 24 h, the compound-containing media was removed and fresh media without compound was added. For continuous exposure to compound, it remained in contact with the cells for the entire incubation period. The dishes were incubated for up to 7 days, media were removed, and the colonies were stained with crystal violet. Colonies containing 50 cells or more were counted. The results were normalized to an untreated control. Plating efficiency for the untreated cells was about 90%. Repeat experiments were carried out to define the cell survival range between 100% and 10^{-3} survival.

4.7. Isolation of efrapeptins and RHMs

The extraction procedure of the 20 L 021172cKZ culture has been described,[5] briefly, crude oils were generated from separate extractions of the broth and mycelia, which were then partitioned between 90% aqueous methanol and hexanes, followed by a 50% aqueous methanol and dichloromethane partition. All preparative and semi-preparative HPLC were reversed-phase (RP) and were carried out using MeCN in H_2O both with 0.1% formic acid. The dichloromethane soluble mycelial extract (TFD, 4.76 g) was fractionated with preparatory RP-HPLC (PREP HPLC 1 in Chart 1) (25–75% MeCN in H_2O over 30 min) generating fractions P1–Pwash. RHM1 of 345 mg and RHM2 of 33.5 mg were purified from P2 (880.5 mg).[5] RHM3 (**3**) was purified via two semi-prep RP-HPLC fractionations (50–88% MeCN in H_2O over 24 min, followed by 60–85% MeCN in H_2O over 15 min) to afford **3** (5.0 mg). Prep fractions P4 (88.4 mg) and Pwash (388 mg) were combined and subjected to semi-prep RP-HPLC (50–75% MeCN in H_2O to 25 min, followed by 10 to 100% MeCN) to afford **4** (34.3 mg).

The TFD (1.89 g) was subjected to another round of prep RP-HPLC (PREP HPLC 2 in Chart 1) (40–100% MeCN in H_2O

over 10 min) to generate fractions P1a–Pwa (Chart 1). P12a (224.3 mg) contained efrapeptins by LC–ESI-MS and was subjected to further fractionation via semi-prep RP-HPLC (40% MeCN in H_2O for 10 min followed by 20 min to 60% MeCN in H_2O) to afford 13 fractions. Compounds of MW 1606 and 1620 were enriched in the combined H5–H6, 1.4 mg, purified by semi-prep RP-HPLC (40–70% MeCN over 25 min). Fractions H6 (10.1 mg) and H7 (17.6 mg) were combined and subjected to semi-prep RP-HPLC (40–60% MeCN in H_2O over 20 min) to afford **1** (3.3 mg). Efrapeptin G was purified in H9, 23.2 mg. A combination of H10 (5.3 mg) and H11 (5.1) was subjected to semi-prep RP-HPLC (45–55% MeCN in H_2O over 10 min) to yield efrapeptin F (1.0 mg) and a mixture of efrapeptins E and H (**2**) (1.7 mg).

4.8. Isolation of destruxins

The filtered culture broth of strain 001103 was extracted with EtOAc three times to give the crude extract (E, 2.0 g). The EtOAc extract was further partitioned by our standard partition procedure[36] to afford *n*-hexane (EFH, 24 mg), CH_2Cl_2 (EFD, 1.6 g), and MeOH extracts (EFM, 184 mg) (Fig. S1, Supplementary data). The EFD extract was applied to a flash column chromatography with CH_2Cl_2/MeOH stepwise gradient as eluant to afford 12 fractions (B1—B12). Fraction B6 (195 mg) eluted with 1% MeOH in CH_2Cl_2 was purified by RP-HPLC with MeOH/H_2O (3:2 to 17:3 linear gradient) as eluant to afford E chlorohydrin (70.4 mg), B (14.0 mg), and four semi-pure fractions, H3, H7, H9, and H10 that were further purified by RP-HPLC with MeOH/H_2O isocratic conditions (H3, 3:2; H7 and H9, 13:7; and H10, 7:3) to afford E2 chlorohydrin (4.8 mg), A (4.7 mg), B2 (1.6 mg), and desmethyl B (2.6 mg), respectively. The isolated six destruxins were identified by comparison of the ^1H and ^{13}C NMR data with the published values.[20,37]

4.9. Efrapeptin Eα (1)

White solid; $[\alpha]_D^{28}$ −2.0 (*c* 0.20, $CHCl_3$), $[\alpha]_D^{27}$ 5.0 (*c* 0.23, MeOH); for ^1H NMR (600 MHz, MeOH-d_4) data see Table S1, Supplementary data. HR-ESI-Q-q-TOF-MS *m/z* 1634.0756 $[M]^+$ (calculated for $C_{82}H_{141}N_{18}O_{16}$, Δ 1.1 mDa).

4.10. Efrapeptin H (2)

White solid; HR-ESI-Q-q-TOF-MS *m/z* 1662.1078 $[M]^+$ (calculated for $C_{84}H_{145}N_{18}O_{16}$, Δ 0.2 mDa).

4.11. RHM3 (3)

White crystalline solid; $[\alpha]_D^{27}$ −52.6 (*c* 0.23, MeOH); for ^1H NMR (500 MHz, DMSO-d_6) and ^{13}C NMR (125 MHz, DMSO-d_6) data see Table 1; HR-ESI-TOF-MS *m/z* 1030.6878 $[M+Na]^+$ (calculated for $C_{51}H_{93}N_9O_{11}Na$, Δ 0.9 mDa).

4.12. RHM4 (4)

White crystalline solid; $[\alpha]_D^{27}$ −33.5 (*c* 0.24, MeOH); for ^1H NMR (500 MHz, DMSO-d_6) and ^{13}C NMR (150 MHz, DMSO-d_6) data see Table 2; HR-ESI-MS *m/z* 1073.7254 $[M+Na]^+$ (calculated for $C_{54}H_{98}N_8O_{12}Na$, Δ 5.7 mDa).

Acknowledgements

This work was supported by the National Institute of Health (RO1 CA 47135), NMR equipment grants NSF-CHE-0342912 and NIH S10-RR19918, and MS equipment grant NIH S10-RR20939. Additional support was provided by the GAANN fellowship to C.M.B. We thank B. Boggess and N. Sevova at Notre Dame for providing FAB-MS and HR data on the efrapeptins, M. Kelley at UCSF for 800 MHz NMR data, and A. Amagata at UCSC for assistance with fungal cultures. The staff of the UT San Antonio Health Sciences Center, Fungus Testing Laboratory, D. A. Sutton and B. Wickes, are acknowledged for fungal IDs. We would also like to thank L. Matainaho of the University of Papua New Guinea for providing collection permit support, the Captain (C. de Wit) and Crew of the *M/V Golden Dawn* for Papua New Guinea field assistance, and W. Aalbersberg for collection permit support in Fiji.

Supplementary data

Structures of destruxins A, B, and B2, desmethyl B, E chlorohydrin, E2 chlorohydrin, and scytalidamides A and B; ^1H NMR and ESI-MS^n for efrapeptin Eα (**1**), ESI-MS^n for efrapeptins E, F, and H (**2**) and compounds with MW of 1606 and 1620; the ^1H and ^{13}C NMR, gCOSY and gHMBC spectra, and ESI-MS^n for **3**, ^1H and ^{13}C NMR, gHMBC at 500 and 800 MHz, and gCOSY spectra for compound **4** are available free of charge via the internet at www.elsevier.com. Supplementary data associated with this article can be found in the online version, at doi:10.1016/j.tet.2007.06.034.

References and notes

1. Bugni, T. S.; Ireland, C. M. *Nat. Prod. Rep.* **2004**, *21*, 143–163.
2. Ebel, R. *Frontiers in Marine Biotechnology*; Proksch, P., Muller, W. E. G., Eds.; Horizon Bioscience: Wymondham, 2006; pp 73–143.
3. In Refs. 1 and 2, 225 and 272, respectively, new natural products from marine-derived fungi are reported. A SciFinder search, 1/12/2007, for new marine-derived fungal natural products in the years 2005 and 2006 yielded 71 additional structures for a total of 568 structures, however, the searches for 2005 and 2006 were not exhaustive, thus the total number of structures is likely to be higher.
4. von Doehren, H. *Advances in Biochemical Engineering/Biotechnology*; Springer: Berlin, Heidelberg, 2004; Vol. 88, pp 217–264.
5. Boot, C. M.; Tenney, K.; Valeriote, F. A.; Crews, P. *J. Nat. Prod.* **2006**, *69*, 83–92.
6. Gupta, S.; Krasnoff, S. B.; Roberts, D. W.; Renwich, J. A. A.; Brinen, L. S.; Clardy, J. *J. Org. Chem.* **1992**, *57*, 2306–2313.
7. Tan, L. T.; Cheng, X. C.; Jensen, P. R.; Fenical, W. *J. Org. Chem.* **2003**, *68*, 8767–8773.
8. Jackson, C. G.; Linnett, P. E.; Beechey, R. B.; Henderson, P. J. *Biochem. Soc. Trans.* **1979**, *7*, 224–226.
9. Bullough, D. A.; Jackson, C. G.; Henderson, P. J. F.; Cottee, F. H.; Beechey, R. B.; Linnett, P. E. *Biochem. Int.* **1982**, *4*, 543–549.
10. Gupta, S.; Krasnoff, S. B.; Roberts, D. W.; Renwick, J. A. A.; Brinen, L. S.; Clardy, J. *J. Am. Chem. Soc.* **1991**, *113*, 707–709.
11. Krasnoff, S. B.; Gupta, S. *J. Chem. Ecol.* **1991**, *17*, 1953–1962.

12. Nagaraj, G.; Uma, M. V.; Shivayogi, M. S.; Balaram, H. *Antimicrob. Agents Chemother.* **2001**, *45*, 145–149.
13. Valeriote, F.; Grieshaber, C. K.; Media, J.; Pietraszkewicz, H.; Hoffmann, J.; Pan, M.; McLaughlin, S. *J. Exp. Ther. Oncol.* **2002**, *2*, 228–236.
14. Crews, P.; Rodriguez, J.; Jaspars, M. *Organic Structure Analysis*; Oxford University Press: New York, NY, 1998; p 8.
15. Papayannopoulos, I. A. *Mass Spectrom. Rev.* **1995**, *14*, 49–73.
16. Ballard, K. D.; Gaskell, S. J. *J. Am. Soc. Mass Spectrom.* **1993**, *4*, 477–481.
17. Fredenhagen, A.; Molleyres, L.; Bohlendorf, B.; Laue, G. *J. Antibiot.* **2006**, *59*, 267–280.
18. The *Scytalidium* ID was based on fatty acid methyl ester analysis, our analysis of this sample was based on phenotypic and sequence analyses as described in Section 4.
19. Gupta, S.; Roberts, D. W.; Renwick, J. A. A. *J. Chem. Soc., Perkin Trans. 1* **1989**, 2347–2357.
20. Yeh, S. F.; Pan, W.; Ong, G. T.; Chiou, A. J.; Chuang, C. C.; Chiou, S. H.; Wu, S. H. *Biochem. Biophys. Res. Commun.* **1996**, *229*, 65–72.
21. Bandani, A. R.; Amiri, B.; Butt, T. M.; Gordon-Weeks, R. *Biochim. Biophys. Acta* **2001**, *1510*, 367–377.
22. Abrahams, J. P.; Buchanan, S. K.; vanRaaij, M. J.; Fearnley, I. M.; Leslie, A. G. W.; Walker, J. E. *Proc. Natl. Acad. Sci.* **1996**, *93*, 9420–9424.
23. Papathanassiu, A. E.; MacDonald, N. J.; Benesura, A.; Vu, H. A. *Biochem. Biophys. Res. Commun.* **2006**, *345*, 419–429.
24. Blagg, B. S. J.; Kerr, T. A. *Med. Res. Rev.* **2006**, *26*, 310–338.
25. Whitesell, L.; Mimnaugh, E. G.; Decosta, B.; Myers, C. E.; Neckers, L. M. *Proc. Natl. Acad. Sci.* **1994**, *91*, 8324–8328.
26. Chen, X. Y.; Bies, R. R.; Ramanathan, R. K.; Zuhowski, E. G.; Trump, D. L.; Egorin, M. J. *Cancer Chemother. Pharmacol.* **2005**, *55*, 237–243.
27. Glaze, E. R.; Lambert, A. L.; Smith, A. C.; Page, J. G.; Johnson, W. D.; McCormick, D. L.; Brown, A. P.; Levine, B. S.; Covey, J. M.; Egorin, M. J.; Eiseman, J. L.; Holleran, J. L.; Sausville, E. A.; Tomaszewski, J. E. *Cancer Chemother. Pharmacol.* **2005**, *56*, 637–647.
28. Zheng, J. B.; Ramirez, V. D. *Br. J. Pharmacol.* **2000**, *130*, 1115–1123.
29. Baur, J. A.; Sinclair, D. A. *Nat. Rev. Drug Discov.* **2006**, *5*, 493–506.
30. Subramanian, B.; Nakeff, A.; Tenney, K.; Crews, P.; Gunatilaka, L.; Valeriote, F. *J. Exp. Ther. Oncol.* **2006**, *5*, 195–204.
31. Jost, M.; Greie, J. C.; Stemmer, N.; Wilking, S. D.; Altendorf, K.; Sewald, N. *Angew. Chem., Int. Ed.* **2002**, *41*, 4267–4269.
32. Jost, M.; Sonke, T.; Kaptein, B.; Broxterman, Q. B.; Sewald, N. *Synthesis* **2005**, 272–278.
33. Soledade, M.; Pedras, C.; Zaharia, L. I.; Ward, D. E. *Phytochemistry* **2002**, *59*, 579–596.
34. Toske, S. G.; Jensen, P. R.; Kauffman, C. A.; Fenical, W. *Tetrahedron* **1998**, *54*, 13459–13466.
35. Kock, M.; Kessler, H.; Seebach, D.; Thaler, A. *J. Am. Chem. Soc.* **1992**, *114*, 2676–2686.
36. Amagata, T.; Rath, C.; Rigot, J. F.; Tarlov, N.; Tenney, K.; Valeriote, F. A.; Crews, P. *J. Med. Chem.* **2003**, *46*, 4342–4350.
37. Gupta, S.; Roberts, D. W.; Renwick, J. A. A. *J. Liq. Chromatogr.* **1989**, *12*, 383–395.